

Inductive Power Charging for Electric Vehicles in Misalignment Conditions

Constantin M. Apostoaia, *Member, IEEE*^{1,2}, Mihai Cernat, *Senior Member, IEEE*²

¹Purdue University Northwest, Hammond, IN, USA, Apostoai@pnw.edu

²Transilvania University of Brasov, Romania, mihaicernat@yahoo.com

Abstract - This research work deals with the challenges and issues facing the misalignment contactless inductive power charging of electric vehicles (EVs). The focus is on analysis and design of the inductive power transfer (IPT) for dynamic (in-motion) charging systems. The computational electromagnetics approach is used here, and a graphical and programming platform is developed capable to link and co-simulate the models of the coupled coils with the models of the external circuitry of the overall IPT system consisting of: high frequency power inverter on the primary coil side, resonant tuning capacitors, diode bridge rectifier on the secondary coil side, DC filtering capacitor and the vehicle battery load.

Cuvinte cheie: *transfer de putere inductiv, cuplare dinamică, încărcare fără contact, analiză cu elemente finite (FEA), software ANSYS.*

Keyword: *inductive power transfer, dynamic coupling, contactless charging, finite element analysis (FEA), ANSYS software.*

I. INTRODUCTION

In recent years, IPT (or wireless) charging of EVs has been the focus of intensive research studies, and the stationary charging systems have successfully been achieved using the IPT technology. More recently, dynamic (or in-motion) charging with IPT technology has been demonstrated for electrification transportation applications such as utility vehicles, electric buses and trams, or electric trains. Much work is still required on analysis, design, prototype development, and testing of IPT systems for dynamic EV charging. Optimization studies are required on related-relevant issues such as: coils magnetic coupling, coils misalignment tolerance and compensation, power electronics converters, and resonant circuitry for dynamic charging systems. The need to understand many challenges facing of in-motion charging of vehicles was recognized in 2012 by the U.S. Department of Transportation [1].

Many studies, implementing the inductive transfer of electrical power between two coils, have been published in the past decade under the high pressure to find new energy storage technologies and extend the driving range of EVs. Many aspects of electric vehicle inductive power transfer have been introduced and discussed in [1], and [2], and a laboratory bench for experimental charging in-motion demonstration has been implemented. In [2] it is shown that when a coil passes across a pair of energized coils, the transmitted power varies with respect to their position, and fluctuations in the power occur. In [3], a hybrid electric vehicle was wireless plug-in powered

using a pair of coupled coils, and the performances were examined at different gaps and different operating frequencies. In [4], a 20 kW wireless power transfer at 400 V/20 kHz was modeled by ANSYS software considering the coupling of the electromagnetic coils model with the external circuit. The energy efficiency for a two-coil wireless power transfer system may be maximized by using the method presented in [5]. For analyzing the power flow in the wireless power transfer it is possible to consider primary (transmitter) coil as the frequency selection stage, to insure the highest mutual flux development and thus to facilitate the power transmission, while the secondary (receiver) coil is a voltage controlled utility network [6]. The development and implementation of a high efficiency wireless power transfer charging system up to 12 kW, integrated into a Toyota RAV4 electric vehicle is presented in [7]. [8] presents a topology that integrates a wireless charging system and the boost converter for the traction drive system. [9] proposes to use the common utility low frequency in anticipation of a higher potential wireless charging for small power EVs.

In order to extend the application of IPT for vehicle charging, the most important issue of coupling power over relatively large gaps has been solved using high frequency (HF) magnetic resonance.

The achievement of high power transfer efficiency is determined by a multitude of influencing factors such as the number of turns of primary and secondary coils, that is the system main component, the coil geometry, the gap and alignment between the coils, or the excitation frequency.

In the end, a good design should lead to a high coupling coefficient, k , with a minimum variation due to predicted changes in air-gap and expected range in lateral misalignment of the pair of coupled coils [10]. The objectives of this study are (i): the FEA based modeling and analysis of the pair of resonant magnetic coupled coils, and (ii): the development of the graphical and programming platform capable to link and simulate the models of the coupled coils in-motion with the models of the external circuitry of the overall IPT system, consisting of: high frequency power inverter on the primary coil side, resonant tuning capacitors, diode bridge rectifier on the secondary coil side, DC filtering capacitor and the vehicle battery load.

The main goal in this research is to complete the study done in the previous work for the stationary IPT system [11], and validate the efficient operation of the new designed system in dynamic regime (in-motion). This objective is achieved by employing the ANSYS

numerical FEA software, and developing a new co-simulation platform based on the two software components, namely ANSYS Maxwell™ and ANSYS Simplorer™ [13]. In this way, the coupled coils parameters, such as the coils resistances, self-inductances, mutual inductance and coupling coefficient, are accurately calculated and extracted from eddy-current and magneto-static solutions in ANSYS Maxwell environment.

The coupled coils design is based on using stranded conductors, series tuned resonant capacitor on the primary coil and a parallel resonant capacitor on the secondary coil side, soft ferrite pad structures, and small thickness non-magnetic shields.

The study in this paper is organized in five sections. In Introduction, the motivation of the simulation platform development was presented, and the work in progress elsewhere was discussed. In the second section, the FEA design of the coupling coils, and considering their longitudinal misalignment, will be examined. The overall IPT charging system description, and aspects of power transfer efficiency are presented in the third section. The simulation results are presented and discussed in the fourth section. The concluding remarks are outlined in the final section.

II. FEA COIL DESIGN

The objective to achieve more accurate coils models, compared to the analytical equivalent coil circuits with constant parameters, is achieved using the ANSYS software. The coil models are created by using the software's own geometry utilities, and then the coil parameters are generated and extracted employing the Magneto-static and Eddy Current solvers available in ANSYS Maxwell.

In our preliminary study [11], two different shapes of the coil pair have been considered, each with various numbers of turns and geometric dimensions. Figs. 1 and 2 illustrate some of these design variants with or without soft ferrite flux guides or aluminum shielding. The primary coil is placed on the ground surface level, and the secondary is mounted underneath the vehicle on its chassis. The gap separating the coils is represented by the car ground clearance.

In Fig. 1(a), each rectangular coil consists of 3 turns of stranded copper wire. The area determined by the most outer turn of primary coil is 0.8 m^2 . For this initial design the obtained coupling coefficient is only $k=0.14$. In Fig. 1(b) a new design is illustrated with two identical coils in size and number of turns: each single layer spiral coil has 3 turns of stranded copper wire. In this new variant, the coupling coefficient is increased to $k=0.36$.

Figs. 2(a) and 2(b) illustrate a new design with two variants. In Fig. 2(a), both coils have the same circular spiral shape, an equal number of 10 turns, and the same geometric size with a median radius of 35 cm. In Fig. 2(b), representing the final improved design, two soft ferrite cores of small thickness and aluminum shield plates have been added.

Here, both primary and secondary coils have the same inner start radius of 15 cm, and a radius change of 2.15 cm per turn. In this case, the primary coil has 7 turns, the secondary 5 turns, and they are 100% aligned.

The parameters of this pair of coils are extracted at 22 kHz operating frequency as follows: $R_1=0.860 \text{ m}\Omega$,

$R_2=0.700 \text{ m}\Omega$, $L_1=19.57 \text{ }\mu\text{H}$, $L_2=13.74 \text{ }\mu\text{H}$, mutual inductance $M=5.24 \text{ }\mu\text{H}$ and the coupling coefficient $k=0.32$, with 150 mm gap between the coils.

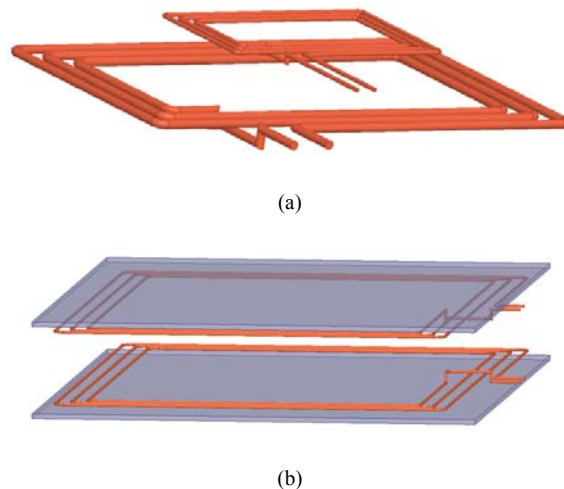


Fig. 1. Maxwell 3D design of loosely coupled coils, 3 turns each, of rectangular shape: (a) $k=0.14$; (b) with ferrite pads, $k=0.36$.

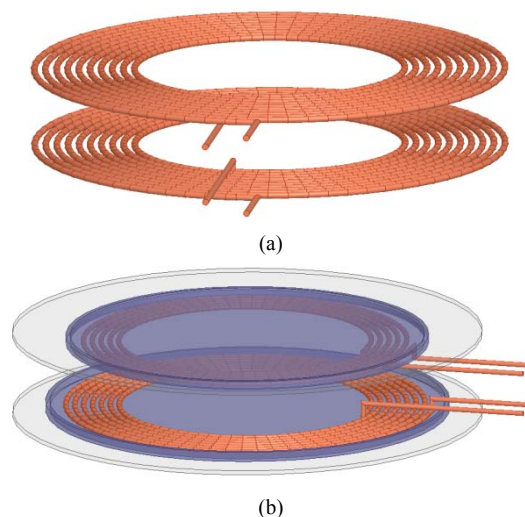


Fig. 2. Maxwell 3D design of loosely coupled of circular shape: (a) 10 turns each coil, $k=0.26$; (b) 7/5 turns with ferrite pads and aluminum shields.

In order to study the effect of the misalignment between these coils a Maxwell 2D design is generated from the 3D model as shown in Fig. 3.

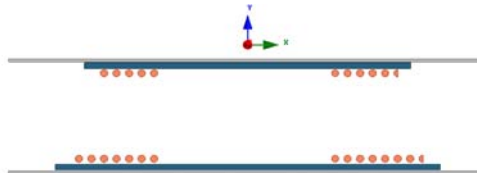


Fig. 3. Maxwell 2D design generated from the coils 3D model shown in Fig. 2(b).

The simulation results of the coils misalignment are presented in section IV of this study. The final 2D design of the coupled coils in Fig. 3 is imported in ANSYS Simplorer for the overall IPT dynamic system model development which is described in the next section.

III. DYNAMIC IPT SYSTEM DESCRIPTION

For a dynamic, charging-in-motion system for EVs, high level of power is required. In this situation, a string of pad-like structures with primary coils are embedded in the roadway and switched synchronously with the motion of the vehicle carrying the secondary coil [1]. In this way, there are always pads in close alignment under the vehicle enabling higher power levels to be transferred. A two-coil primary with moving secondary IPT system exemplification is shown in Fig. 4.

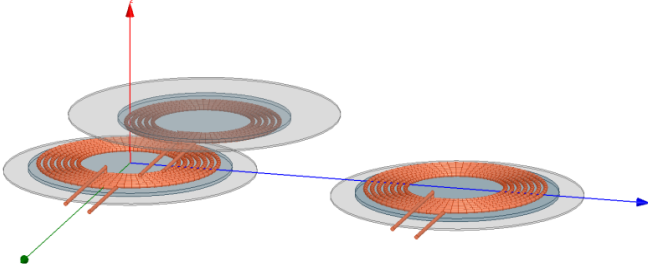


Fig. 4. A two-coil primary with moving secondary in a dynamic IPT system.

The modeling and co-simulation of the overall IPT system is implemented using the dynamic link between ANSYS's Maxwell and Simplorer environments. The Simplorer block diagram realization of the IPT charger schematic is illustrated in Fig. 5.

The following models of the IPT system components are built and added into Simplorer external circuit simulator, besides the imported Maxwell 2D model of the coupling coils previously designed: the input DC power supply, the high frequency H-bridge inverter, the series tuned resonant capacitor on the primary coil side and the parallel capacitor on the secondary coil side, the diode

bridge, the DC filtering capacitor, and the vehicle battery loading.

A. H-bridge Power Inverter

The voltage of the power inverter is adjusted using the input DC power supply (V_{din}) which actually represents the grid voltage full-wave rectified and filtered (not represented in Fig. 5). This input voltage of the high frequency inverter, the switching frequency and duty cycle, determine the amount of power transferred to the secondary coil. The H-bridge inverter synthesizes the switching voltage V_1 across the primary side of the pair of coupled coils, and drives the current excitation I_1 in the primary coil. In various publications, the operating frequency of the IPT system is recommended in a range of 10 to 50 kHz for the poorly coupled coils ($k < 0.5$). The choice of the power inverter operating frequency is $f = 22$ kHz, as in the previous work [11]. This value is close to the one employed in Oak Ridge National Laboratory (ORNL) experimental setups, with good experimental reported results [1, 2].

B. Coupled Inductors Circuits

The pair of coupled coils of the IPT system represents an air-core transformer with very small coil resistances, high leakage inductances, and a small magnetizing inductance. Therefore for the correct circuit analysis, it is desirable to modify the model of the ideal transformer for unity ($k=1$) coupled inductors (Fig. 6(a)), to account for loosely coupling ($k < 1$) situation which is the case of the pair of coils of the IPT system (Fig. 6(b)).

The connected load resistance R_L shown in Fig. 6 on the secondary coil side represents the battery equivalent resistance seen on the AC side of the diode bridge charging rectifier in Fig. 5, [11].

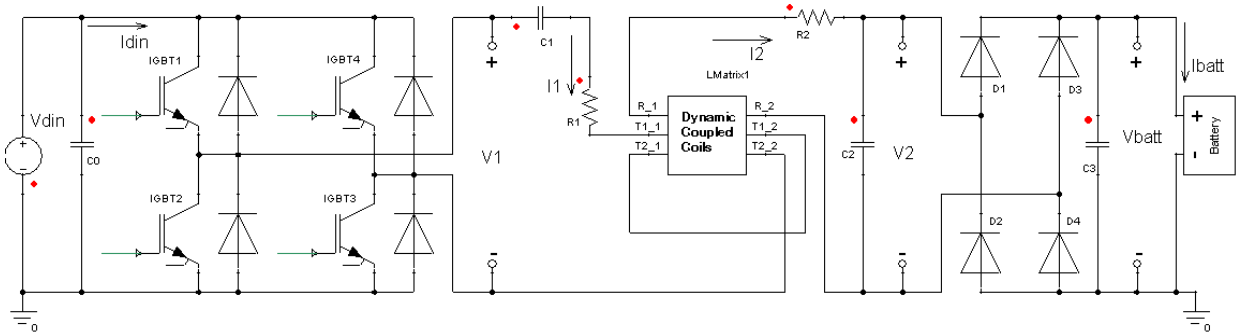


Fig. 5. Resonant IPT dynamic system model built in Simplorer.

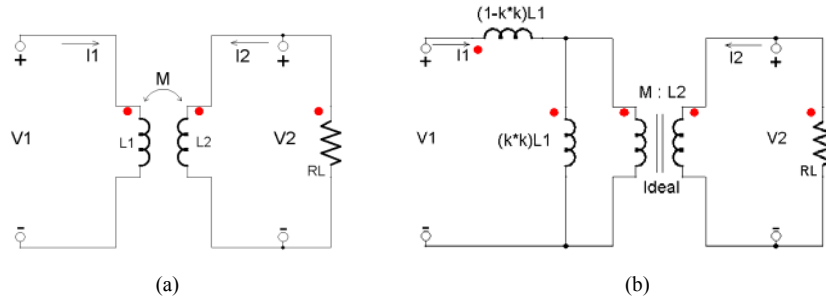


Fig. 6. (a) Unity coupled inductors with a connected load resistance; (b) A model of the coupled inductors ($k < 0.5$) with an ideal transformer.

For the ideal unity coupling (Fig. 6(a)), with mutual inductance M , the circuit equations in the frequency domain are given by,

$$\begin{bmatrix} \underline{V}_1 \\ \underline{V}_2 \end{bmatrix} = \begin{bmatrix} j\omega L_1 & j\omega M \\ j\omega M & j\omega L_2 \end{bmatrix} \begin{bmatrix} \underline{I}_1 \\ \underline{I}_2 \end{bmatrix} \quad (1)$$

Solving for \underline{I}_2 from the Eq. (1)

$$\underline{I}_2 = \frac{\underline{V}_2}{j\omega L_2} - \frac{M}{L_2} \underline{I}_1 \quad (2)$$

Substituting Eq. (2) in Eq. (1), the voltage equation on the primary side is rewritten as,

$$\underline{V}_1 = j\omega L_1 \left(1 - \frac{M^2}{L_1 L_2} \right) \underline{I}_1 + \frac{M}{L_2} \underline{V}_2 \quad (3)$$

In the non-idealized coupled coils, $L_1 L_2 > M^2$ with the coupling coefficient $k < 1$. Substituting the mutual inductance $M = k\sqrt{L_1 L_2}$ in Eq. 3, we have

$$\begin{aligned} \underline{V}_1 &= j\omega L_1 (1 - k^2) \underline{I}_1 + \frac{M}{L_2} \underline{V}_2 = \\ &= j\omega L_1 \sigma \underline{I}_1 + \frac{M}{L_2} \underline{V}_2 \end{aligned} \quad (4)$$

where σ is the leakage factor given by:

$$\sigma = 1 - \frac{M^2}{L_1 L_2} = 1 - k^2. \quad (4a)$$

The equivalent circuit to model Eq. (4) is illustrated in Fig. 6(b). The term $j\omega L_1 \sigma \underline{I}_1$ is the voltage drop due the large leakage inductance $(1 - k^2)L_1$ and the transformer action is indicated by the second term, $(M/L_2)\underline{V}_2$ with the transformer ratio given by M/L_2 .

The remaining small inductance, $k^2 L_1 = L_1'$, together with L_2 and M , forms a unity coupling system, satisfying the condition $M^2 L_2 = L_1'$ [12].

Our coupled inductors model represents the case of a moving secondary conducting loop in a time-varying magnetic field produced by the primary (transmitter) coils. The induced emf in the secondary (receiver) coil is the sum of a transformer component and a motional component written as,

$$V_{emf} = V_{emf}^{tr} + V_{emf}^m = - \int_S \frac{\partial \bar{B}}{\partial t} \cdot d\bar{S} + \oint_C (\bar{v} \times \bar{B}) \cdot d\bar{l} \quad (5)$$

Compared to the secondary voltage V_2 , induced at the operation frequency of 22 kHz, with a peak of 68 V (Fig.5), the motion-induced emf component can be neglected. Considering, for example, a vehicle high speed of 60 miles/hour, with an average radius of 23 cm of the moving secondary loop perfectly aligned with a primary coil, and the mid gap flux density of 3 mT obtained in our model (Fig.8), the maximum value of the motion-induced

emf, V_{emf}^m , is about only 105 mV, which is ignorable compared to the component of the voltage induced by transformer action.

C. Efficiency Considerations of the IPT System

In this study, the final design variant of the coupled coils illustrated in Fig. 2(b) is considered with the following parameters: $R_1=0.860$ m Ω , $R_2=0.700$ m Ω , $L_1=19.57$ μ H, $L_2=13.74$ μ H, mutual inductance $M=5.24$ μ H, and the coupling coefficient $k=0.32$ with a 150 mm air gap.

As a measure of the efficient design of an inductor, its quality factor Q can be employed. It is known that the Q factor of an inductor is the ratio of the inductive reactance to its unwanted wire resistance at the operation frequency, given by, $Q=\omega L / R$. A very high Q value is desirable in IPT systems, so that small losses are produced. The value of the quality factor of the secondary coil, in this work, is about $Q=2700$, at 22 kHz, that means the wire resistance is negligible compared to the secondary inductive reactance. Thus, the ohmic losses are drastically reduced and the secondary coil output voltage is mostly applied as desired to the load resistance, R_L shown in Fig. 6. Therefore, the best efficiency is obtained with $R_L \gg R_2$, [11].

The practical evaluation of the dynamic IPT system efficiency is limited by one important factor: the real coupling coefficient k , which cannot be directly measured and must be derived. The analytical expression of the coupling coefficient $k = M\sqrt{L_1 L_2}$, cannot capture the effects of lateral or angular misalignments which are expected in dynamic, charging in-motion systems for electric vehicles. If experimental open secondary test results are available, the coupling coefficient can be derived according to the transformer ratio (replacing M/L_2 in Eq. (4)) given by,

$$V_1/V_2 = k\sqrt{L_1/L_2} \quad (6)$$

with measured output/input voltages and the self inductances of the coupled coils system.

Referring to Fig. 6(b), the load resistance seen looking into primary is given by the impedance transformation property (reflection to primary side),

$$R_L' = k^2 \frac{L_1}{L_2} (R_2 + R_L), \quad (7)$$

where the small secondary coil resistance is not neglected.

Again, the best efficiency is obtained with $R_L' \gg R_1$, in order to reduce the primary coil ohmic losses and most of the power to be transmitted to the load. To determine a high quality factor Q_1 of the primary coil by design, and taking Eq. (7) into consideration, the following restriction should be also met,

$$Q_1 \gg \frac{\omega L_1}{k^2 \frac{L_1}{L_2} (R_2 + R_L)} \quad (8)$$

Both, the quality (factors) of the coils Q and the quality of the magnetic circuit coupling k provide the best way to make a more efficient inductive power transfer system.

High quality Q factors determine also a narrow range of frequencies of resonant circuits. This becomes critical for the IPT system where both coils must resonate with more precision at the same frequency ω_0 . The goal is to determine the compensating capacitances of the external capacitors, C_1 and C_2 , added to accurately tune the circuit and create the resonance condition to maximize the transferred power, (Fig. 5):

$$C_1 = \frac{1}{\omega_0^2(1-k^2)L_1}; \quad C_2 = \frac{1}{\omega_0^2 L_2} \quad (9)$$

The tuned capacitors are determined from the resonance conditions $\text{Im}\{\mathbf{Z}_{1,2}\}=0$, where $\mathbf{Z}_{1,2}$ are the equivalent impedances of the respective RLC resonant circuits, and using the coils design extracted data, L_1 and L_2 , [11].

IV. SIMULATION RESULTS

The IPT system simulation results have been generated using the platform built in ANSYS Maxwell/Simplorer (Fig. 5). The parameters of the designed pair of coils have been extracted using the Maxwell/Eddy Current solver at 22 kHz, and presented in sections II and III.

The main dimensions of the pads structures are illustrated in Fig. 7, where: the aluminum shield plates diameters, $D_1=82$ cm for both primary and secondary coils, the ferrite cores diameters, $D_2=66$ cm on primary side and 56 cm on secondary side, and coils average diameters, $D_3=45$ cm for primary, and 41 cm for the secondary coil.

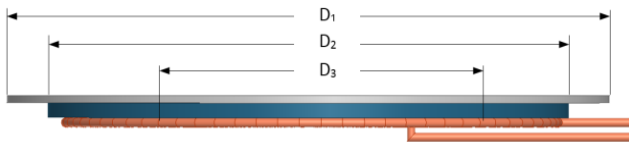


Fig. 7. Main dimensions of coil pad structure.

In the initial simulation of the dynamic charging, the considered IPT system consists of two identical primary coils and a moving secondary in the direction of the vehicle travel, with a constant vertical gap of 150 mm. The considered voltage of the vehicle battery is 80 V, and the required charging power is 1.5 kW, for this IPT charging system.

The horizontal sliding of the secondary coil, on top of the two primary coils, is performed in 4 steps, 250 mm each. That is, the sliding starts from a full (100%) alignment position with the first primary coil to a final complete (100%) overlap with the second primary coil. Fig. 8 illustrates the magnetic field intensity vector in the median position of the secondary coil between the two primary coils, when the transferred power drops to its minimum value during the sliding process. In Fig. 8, the magnitude of the field intensity vector, H , is about 7 kA/m in the mid gap over the primary coil.

Fig. 9 illustrates the magnitude of flux density, B , when the secondary coil is completely aligned with the second primary coil. In the mid gap over the second primary coil, the magnitude of flux density B is about 3 mT.

The variation of the magnetic coupling coefficient, k , in the gap range of 9-21 cm, and with a secondary coil sliding in the range of 0-60 cm, is shown in Fig. 10.

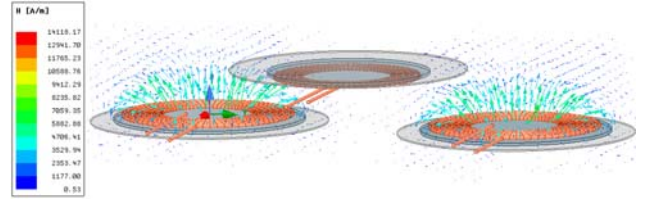


Fig. 8. Magnetic field of two primary coils and the secondary coil moving in horizontal y-direction.

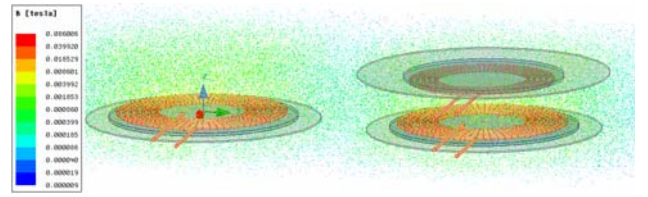


Fig. 9. Magnetic flux density of the coils with the secondary coil 100% aligned with the 2nd primary.

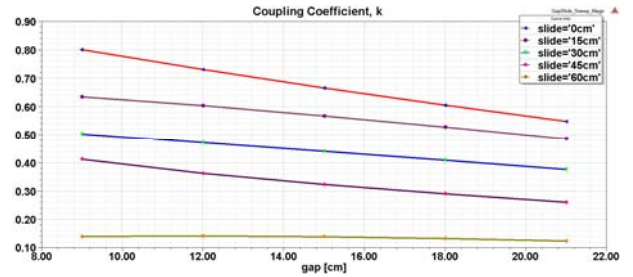


Fig. 10. Coupling coefficient, k , vs. gap, with sliding as parameter.

For a fix vertical gap of 15 cm between the coils, the coupling k value drops from a tight coupling of about 0.68, at the perfect coils alignment, to a loosely coupling of about 0.35 at a 45 cm horizontal sliding in the traveling vehicle direction.

If the slide reaches 60 cm from the null position, the coupling remains almost constant at a low value of about 0.2 regardless the gap variation (Fig. 10).

Figure 11 illustrates the variation of the mutual inductance, M [μH], in the gap range of 9-21 cm, and with a secondary coil sliding in the range of 0-60 cm.

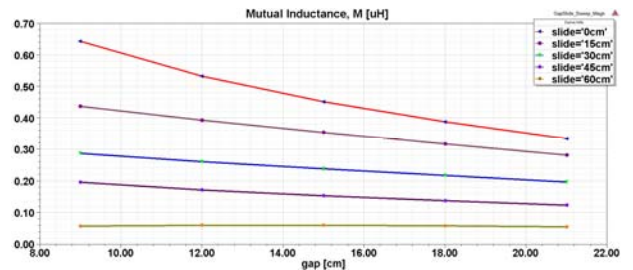


Fig. 11. Mutual inductance, M [μH], vs. gap with sliding as parameter.

Considering the same fix vertical separation of 15 cm between the coils, the value of the mutual inductance drops 20% at a horizontal misalignment of 15 cm, 40% at 30 cm, a significant 64% at 45 cm, and a critical 84% at 45 cm horizontal misalignment (Fig. 11).

Figure 12 illustrates the input-output powers obtained with the IPT system described in this study (Fig. 5).

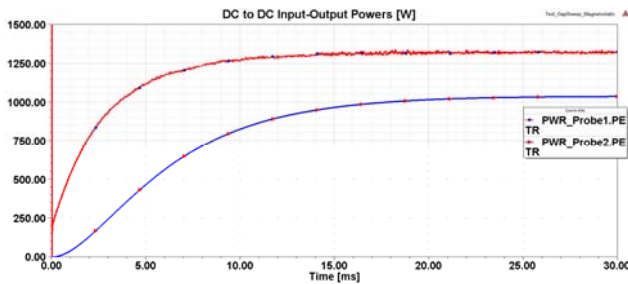


Fig. 12. DC input and DC output powers of the IPT system (Fig. 5).

Figure 13 shows the 77% validated overall efficiency of the IPT system, determined from the DC input of the power inverter to the DC output of the rectifier charging the battery.



Fig. 13. Overall DC-to-DC power transfer efficiency.

V. CONCLUSION

In this study, a computational electromagnetics approach is employed for the modeling and analysis of a dynamic contactless inductive charging system for electric vehicles. The modeling and simulation at the system level is based, here, on the use of ANSYS Maxwell 3D for the accurate design and parameters extraction of the pair of magnetically coupled coils and for their 2D model generation. The ANSYS Simplorer software component allowed the dynamic link between the IPT system external circuitry and the 2D FEA model of the coupled coils.

The magnetic field intensity and flux density simulation results are presented and discussed for the system of two-coil primary and a moving secondary coil.

A parametric sweep has been performed to reveal the modification of the mutual inductive coupling, in terms of k and M , with respect to the variation of the vertical gap and the horizontal sliding between the coils. The obtained IPT system input and output powers and the overall DC-to-DC efficiency simulation results are presented.

This study, together with the preliminary work [11], confirms the transferred DC output power corresponding to overall DC-to-DC efficiency of 77%, reported in experimental tests at 22 kHz operation in reference [2].

ACKNOWLEDGMENT

Source of research funding in this article: Research program of Purdue University Northwest.

Contribution of authors:

Firs author – 50%

First coauthor – 50%

Received on July 15, 2018

Editorial Approval on September 3, 2018

REFERENCES

- [1] J.M. Miller, P.T. Jones, Jan-Mou Li, O.C. Onar, "ORNL Experience and Challenges Facing Dynamic Wireless Power Charging of EV's," *IEEE Circuits and Systems Magazine*, pp. 40-53, Second Quarter 2015, DOI: 10.1109/MCAS.2015.2419012.
- [2] O.C. Onar, J.M. Miller, S.L. Campbell, C. Coomer, C.P. White, L.E. Seiber, "A novel wireless power transfer for in-motion EV/PHEV Charging," *Proc. 2013 28th Annu. IEEE Applied Power Electronics Conf. Exposition (APEC)*, Mar. 17–21, 2013, pp. 3073–3080, DOI: 10.1109/APEC.2013.6520738.
- [3] O.C. Onar, J.M. Miller, S.L. Campbell, C. Coomer, C.P. White, L.E. Seiber, "Oak Ridge National Laboratory wireless power transfer development for sustainable campus initiative," *Proc. IEEE Transportation Electrification Conference and Expo (ITEC)*, pp. 1-8, June 2013, Dearborn, MI, DOI: 10.1109/ITEC.2013.6574506.
- [4] T. Koga, "Wireless Power Transfer for EV", ANSYS Regional Conferences, 2011.
- [5] W.X. Zhong, S.Y.R. Hui, "Maximum Energy Efficiency Tracking for Wireless Power Transfer Systems", *IEEE Transactions on Power Electronics*, vol. 30, No.7, pp.4025-4034, July 2015, DOI: 10.1109/TPEL.2014.2351496.
- [6] J.M. Miller, O.C. Onar, M. Chinthaveli, "Primary-side Power Flow Control of Wireless Power Transfer for Electric Vehicle Charging," *IEEE J. Emerging Sel. Topics Power Electron.*, vol. 3, no. 1, pp. 147–162, March 2015, DOI: 10.1109/JESTPE.2014.2382569.
- [7] O.C. Onar, et al., "A High-Power Wireless Charging System Development and Integration for a Toyota RAV4 Electric Vehicle," Oak Ridge National Laboratory, Contract with the U.S Department of Energy, No. DE-AC05-00OR22725.
- [8] M. Chinthaveli, et. all, "Integrated Charger with Wireless Charging and Boost Functions for PHEV and EV Applications," Oak Ridge National Laboratory, Contract with the U.S Department of Energy, No. DE-AC05-00OR22725.
- [9] H. Ishida, H. Furukawa, T. Kyoden, "Development of Design Methodology for 60 Hz Wireless Power Transmission System," *IEEJ Journal of Industry Applications*, Vol. 5 No. 6, pp. 429-438, 2016, DOI: 10.1541/ieejia.5.429.
- [10] J.T. Boys and G.A. Covic, "IPT Fact Sheet Series: No.1 – Basic Concepts", Department of ECE, The University of Auckland, 2012.
- [11] C.M. Apstoiaia, M. Cernat, "The Inductive Power Transfer System for Electric Vehicles", *2017 International Conference on Optimization of Electrical and Electronic Equipment (OPTIM) & 2017 Intl Aegean Conference on Electrical Machines and Power Electronics (ACEMP)*, May 25-27, 2017, Brasov Romania, DOI: 10.1109/OPTIM.2017.7974973
- [12] R.A. DeCarlo and Pen-Min Lin, *Linear Circuit Analysis*, Oxford University Press (book, 1008 pages).
- [13] *** ANSYS Maxwell/Simplorer, components of ANSYS (Ansoft) software v.16, USA.
- [14] J.M. Miller, O.C. Onar, C.P. White, S. Campbell, C. Coomer, L.E. Seiber, R. Sepe, A. Steyerl, "Demonstrating Dynamic Wireless Charging of an Electric Vehicle: The Benefit of Electrochemical Capacitor Smoothing," *IEEE Power Electronics Magazine*, vol. 1, no. 1, (inaugural issue), Mar. 2014, pp. 12–24, DOI: 10.1109/MPEL.2014.2300978.

- [15] M. Budhia, J.T. Boys, G.A. Covic, C.-Y. Huang, "Development of a single-sided flux magnetic coupler for electric vehicle IPT charging systems," *IEEE Transactions on Industrial Electronics*, vol. 60, No. 1, pp. 318-328, January 2013, DOI: 10.1109/IE.2011.2179274.
- [16] J.M. Li, O.C. Onar, M. Starke, P.T. Jones, "Coupling electric vehicles and power grid through charging-in-motion and connected vehicle technology," in *Proc. IEEE Int. Electric Vehicle Conf. 2014 (IEVC 2014)*, Florence, Italy, Dec. 17-19, 2014, DOI: 10.1109/IEVC.2014.7056218.
- [17] S. Chopra, P. Bauer, "Driving range extension of EV with on-road contactless power transfer – a case study," *IEEE Trans. Ind. Electron.*, vol. 60, no. 1, pp. 329-338, Jan. 2013, DOI: 10.1109/TIE.2011.2182015.
- [18] O.C. Onar, M. Chinthavali, J.M. Miller, "A wireless power transfer system with active rectification & recent progress of ORNL WPT system development," in *Proc. 2nd Conf. Electric Roads and Vehicles (CERV'13)*, Feb. 4-5, 2013, Park City, UT, published in *IEEE Journal of Emerging and Selected Topics in Power Electronics*, Vol.: 3, Issue: 1, March 2015, DOI: 10.1109/JESTPE.2014.2382569.
- [19] G.A. Covic, J.T. Boys, "Modern trends in inductive power transfer for transportation applications," *IEEE J. Emerging Sel. Topics Power Electron.*, vol. 1, no. 1, pp. 28-41, Mar. 2013, DOI: 10.1109/JESTPE.2013.2264473.
- [20] M.B. Scudiere, J.W. McKeever, J.M. Miller, "Design of wireless power transfer for stationary and moving hybrid electric vehicles," *SAE World Congress*, 2011-01-0354, April 2011, Detroit, MI.
- [21] G.A. Covic, M.L.G. Kissin, D. Kacprzak, N. Clausen, H. Hao, "A bipolar primary pad topology for EV stationary charging and highway power by inductive coupling," *Proc. IEEE Energy Conversion Congress and Exposition (ECCE'11)*, pp. 1832-1838, September 2011, Phoenix, AZ, DOI: 10.1109/ECCE.2011.6064008.
- [22] Y. Nagatsuka, N. Ehara, Y. Kaneko, S. Abe, T. Yasuda, "Compact contactless power transfer system for electric vehicles," *Proc. International Power Electronics Conference (IPEC'10)*, pp. 807-813, June 2010, Sapporo, Japan, DOI: 10.1109/IPEC.2010.5543313.
- [23] K. Kobayashi, N. Yoshida, Y. Kamiya, Y. Daisho, S. Takahashi, "Development of a non-contacting rapid charging inductive power supply system for electric-driven vehicles," *Proc. IEEE Vehicle Power Propulsion Conf.*, Lille, Sept. 1-3, 2010, pp. 1-6.
- [24] T. Imura, H. Okabe, Y. Hori, "Basic experimental study on helical antennas of wireless power transfer for electric vehicles by using magnetic resonant couplings," *Proc. IEEE Vehicle Power and Propulsion Conference (VPPC'09)*, pp. 936-940, September 2009, Dearborn, MI, DOI: 10.1109/VPPC.2009.5289747.
- [25] J. Shin, et al, "Design and Implementation of Shaped Magnetic-Resonance-Based Wireless Power Transfer System for Roadway-Powered Moving Electric Vehicles," *IEEE Transactions on Industrial Electronics*, vol.61, No.3, pp.1179-1192, March 2014, DOI: 10.1109/TIE.2013.2258294.
- [26] M. Jung, et al, "Multimode Charging of Electric Vehicles", *Proc. PCIM Europe 2016*, pp. 401-409, ISBN 978-3-8007-4186-1, 2016.
- [27] R.K. Jha, St. Giacomuzzi, G. Buja, M. Bertoluzzo, M.K. Naik, "Efficiency and power sizing of SS vs. SP topology for wireless battery chargers", *2016 IEEE International Power Electronics and Motion Control Conference*, Varna, Bulgaria, 25-30 September, 2016, pp/ 1014-1019, DOI: 10.1109/ EPEPEMC.2016.7752133.